F. Kremer, M. Treß, E.U. Mapesa

Broadband Dielectric Spectroscopy Using Nanostructured Electrode Arrangements

Dielectric measurement techniques [1–4] are distinguished by the fact that their sensitivity increases with decreasing thickness of the sample capacitor and hence decreasing amount of sample material. In order to benefit from this unique principal advantage, the technological challenge has to be resolved how to apply an electric field to a nanometric and, if so, submolecular layer of molecules in a capacitor-like arrangement. It is evident that the conventional approach of evaporating a metal counterelectrode on the molecules under study is no longer applicable as this would immediately result in electric shorts.

The Novocontrol NanoKit opens a novel avenue for the study of molecular relaxations and charge transport on nanometric length scales even down to layers of isolated molecules anchored on a surface. To this end, we use nanostructured electrode arrangements with highly insulating SiO_2 spacers, exhibiting heights down to (100 ± 10) nm. Highly doped ($\rho \approx 0.002\,\Omega$cm) Si dies, cut out of ultraflat wafers with rms roughness of ≈ 0.5 nm, are used as electrodes. The molecules under study are deposited on the substrate (plane die) either by spincoating or by Dip-Pen-Nanolithography (DPN). A sample capacitor is completed by covering the plane die which carries the sample by the upper die which is equipped with nanostructured insulating spacers. Evidently, preparations of this type require appropriate conditions like clean rooms or clean benches. Since the surface-to-volume ratio in nanometric samples is extraordinarily high, effects due to the adsorption of, e.g., water or organic pollutants from ambient air must be considered with great care. In the Novocontrol NanoKit, the details of preparation are described thoroughly, thus making measurements of this type a straightforward endeavour and - after a short training - easily possible. Potential pitfalls in the preparation of thin molecular layers are discussed.

Installation Requirements

Preparations of capacitors with thickness down to 100 nm require clean room conditions or at least a flow box with filtered air. We recommend the usage of filters of grade H14, ensuring the removal of more than 99,995 % of dust particles. Commercial systems are offered, e.g., by spetec Ges. für Labor- und Reinraumtechnik mbH (`http://www.spetec.de`), erlab D.F.S S.A.S (`http://captair.com`) or Bleymehl Reinraumtechnik GmbH (`http://www.bleymehl.com`).

Capacitor Arrangements

All preparative steps have to be carried out in a clean room or on a clean bench. To remove organic absorbents, both the plane and the nanostructured dies are rinsed in acetone (VLSI grade) and ultra-sonicated for 10 minutes followed by drying in pure nitrogen. Low molecular weight probes or polymers are deposited on the plane dice by spincoating at a rotation frequency of, e.g., 50 rps.
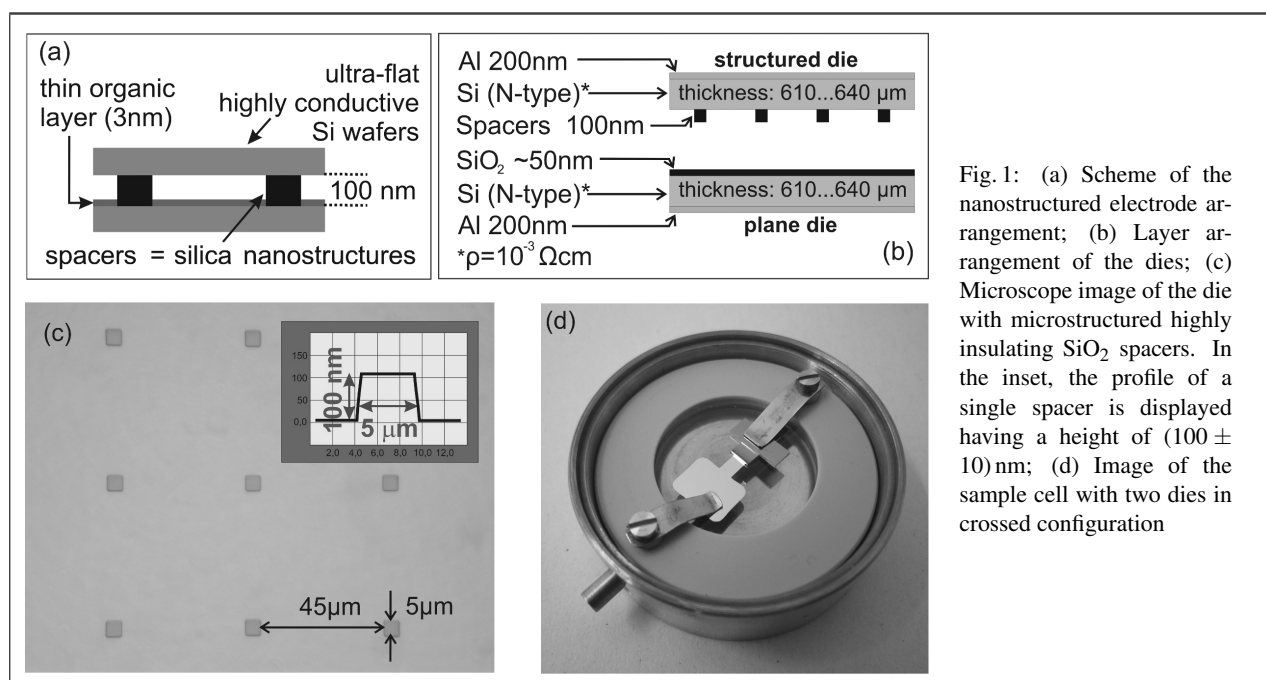

Fig. 1: (a) Scheme of the nanostructured electrode arrangement; (b) Layer arrangement of the dies; (c) Microscope image of the die with microstructured highly insulating SiO_2 spacers. In the inset, the profile of a single spacer is displayed having a height of (100 ± 10) nm; (d) Image of the sample cell with two dies in crossed configuration

Preparation of Nanostructured Capacitor Arrangements

In Dip-Pen-Nanolithography (DPN), small numbers of molecules are transfered to the plane dies by use of an appropriate cantilever. Since both techniques, i.e., DPN and spin coating, operate with solutions of the molecules of interest, subsequent removal of the solvent necessitates annealing of the sample at elevated temperatures in an oil-free vacuum (about 10^{-6} mbar) for an extended period of time. In the final step, the two dies are attached to each other as indicated in Fig. 1a and mounted in the sample cell (Fig. 1d). The latter fits directly into the usual Novocontrol sample cell.

Preparation Hints

Despite the cleaning with 99.99 % acetone and by ultrasonication, organic pollutants might still remain on the surfaces of the plane and nanostructured dies. In this case, it is recommended to repeat the cleaning process and to employ a plasma cleaner or CO_2 snow jet if available. If an electric short is observed one should separate the plane and the nanostructured dies and bring them in contact at a slightly different position again. Both plane and the nanostructured dies can be reused after thorough cleaning.

Examples of Experimental Application

To demonstrate the scope of the nanostructured electrode arrangement [5–8], two experimental examples are briefly presented in the following: (i) the investigation of the segmental and chain dynamics of thin layers of cis-1,4-polyisoprene, and (ii) the measurement of the glassy dynamics of "semi-isolated" poly-2-vinylpyridine polymer coils. In both cases the samples were prepared from dilute chloroform solutions and spin-cast onto the supporting silicon electrode. The layer thickness is adjusted via variation of the concentration; highly dilute solutions yield (semi-) isolated polymer coils. After the deposition of the polymer, the sample is covered by the top electrode and annealing in a high oil-free vacuum (10^{-6} mbar) at ca. 50 K above T_g is commenced for about 24 h. Measurements performed after the application of this procedure have been proven to deliver fully reversible results [2]. Cis-1,4-polyisoprene is a suitable candidate for dielectric investigation since the molecular dipole moments of its segments have a component which adds up along the backbone of the chain. The result is a cumulative dipole moment which corresponds to the end-to-end vector of the chains and makes the dynamics of the whole chain accessible by dielectric spectroscopy.
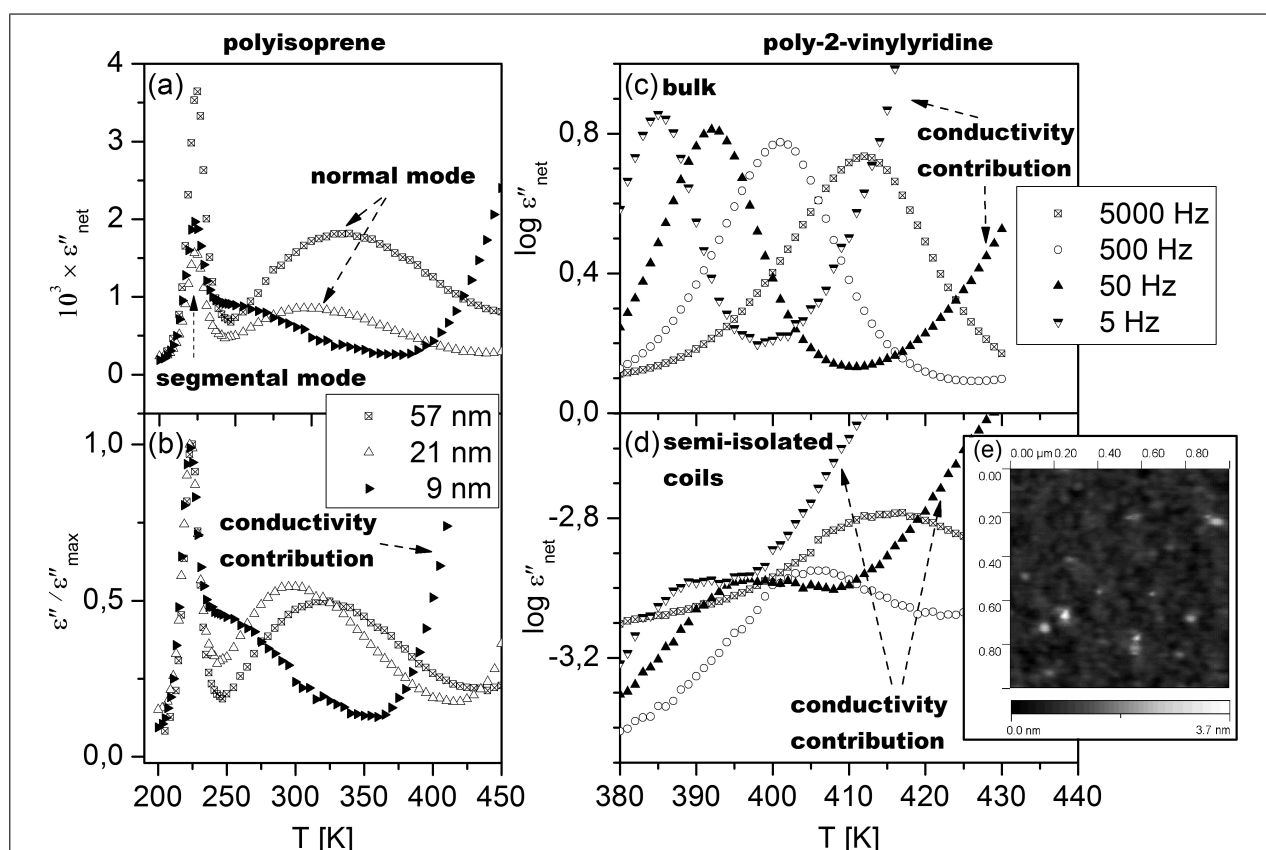

Fig. 2: Dielectric loss ε''_{net} versus temperature at a frequency of 120 Hz for cis-1,4-polyisoprene of molecular weight Mw = 75 kg/mol in thin layers with thicknesses as indicated (a). The same data is shown normalized w.r.t. the maximum loss value of the segmental mode in (b). The high temperature wing is a conductivity contribution. Dielectric loss ε''_{net} versus temperature of poly(2-vinyl pyridine) (MW = 1 700 kg/mol) bulk (c) and semi-isolated coils (d) measured at several frequencies as indicated. The former is prepared conventionally in a capped arrangement with evaporated electrodes while the latter is experimentally accessible only by use of the nano-structured electrode arrangement. (e) shows an AFM (heights) image of the semi-isolated coils on the silicon electrode.

Fig. 2a shows the dielectric loss versus temperature of thin polyisoprene layers; two relaxation processes assigned to glassy dynamics (segmental mode) and chain motion (normal mode) are visible. The curves normalized with respect to the maximum value of the loss, presented in fig. 2b, clarify that: (i) the segmental mode is unaffected by the confinement to a thin layer, and (ii) the normal mode is shifted to lower temperatures, approaching the segmental mode, with decreasing layer thickness. While the dynamic glass transition is independent of film thickness (at least in the range studied here), it is clear that the conformation of the chain changes considerably as underscored by the latter observation. Poly-2-vinylpyridine with its considerably large dipole moment is suitable for experiments which involve very small amounts of material - this is the case when the limit of non-interacting polymer chains is approached. The volume of the sample capacitor is determined by the height of the nano-structures (and the electrode area, of course), while the polymer chains have to be placed on the substrate in such a way that they are well separated. Consequently, the filling ratio of the capacitor is in the per mill range which reduces the signal intensity by about three decades. Experimentally, it has been achieved to measure the glassy dynamics of "semi-isolated" P2VP polymer coils where "semi-isolated" means that there are non-interacting droplets which consist of about 5…10 polymer chains (an atomic force microscope image is presented in fig. 2e). Fig. 2d displays the corresponding loss curves versus temperature in comparison with a bulk sample (fig. 2c). A refined analysis unravels that the peak position of the semi-isolated coils is increased by approx. 5K compared with the bulk. This corresponds to about one decade reduction of the mean relaxation rate which can be assigned to an attractive interaction of the pyridine rings with the native silicon oxide layer of the supporting electrode.

References

[1] A. Serghei and F. Kremer, Rev. Sci. Instrum. 79, 026101 (2008).

[2] A. Serghei and F. Kremer, Macromol. Chem. Phys. 209, 810 (2008)

[3] A. Serghei, H. Huth, C. Schick and F. Kremer, Macromolecules 41 (10), 3636 (2008)

[4] F. Kremer, A. Serghei, J.R. Sangoro, M. Tress and E. U. Mapesa, IEEE Transactions on Dielectrics and Electrical Insulation, (2009) DOI: 10.1109/CEIDP.2009.5377717

[5] E.U. Mapesa, M. Erber, M. Treß, K.-J. Eichhorn, A. Serghei, B. Voit and F. Kremer, Europ. Phys. J. - Special Topics 189, 173-180 (2010), DOI: 10.1140/epjst/e2010-01320-2

[6] M. Erber, M. Treß, E.U. Mapesa, A. Serghei, K.-J. Eichhorn, B. Voit and F. Kremer Macromolecules 43, 7729 (2010), DOI: 10.1021/ma100912r

[7] M. Treß, M. Erber, E.U. Mapesa, H. Huth, J. Müller, A. Serghei, C. Schick, K.-J. Eichhorn, B. Voit and F. Kremer, Macromolecules 43, 9937-9944 (2010) DOI: 10.1021/ma102031k

[8] F. Kremer, E.U. Mapesa, M. Tress, Proceedings of the NATO Advanced Research Workshop in Perpignan, September 2011, in press (2012).

F. Kremer[1], M. Treß, E.U. Mapesa
Universität Leipzig
Institut für Experimentelle Physik I
Linnéstraße 5
04103 Leipzig
Germany
[1]kremer@physik.uni-leipzig.de

C. Daran-Daneau, E. David, M. Fréchette, and S. Savoie

Correspondance of Dielectric Response in Time and Frequency Domains: A Case Study of PE Nanocomposites Containing Nanoclay

Dielectrics are at the core of high-voltage insulation systems, design and performance. Thus, the need to characterize the dielectric responses of these polarizable materials in various contexts and conditions is essential. This is particularly true for advanced dielectrics, for instance nanodielectrics [1], which require detailed studies.

Broadband Dielectric Spectroscopy (BDS) is a powerful tool and may reveal particular and useful features, as its scrutiny spans a large spectrum of excitation frequencies. However, at low frequencies, BDS may suffer some drawbacks, e.g., measurement time and (complicated) sample charging. These restrictions are especially relevant for our purposes since interfacial relaxation occurs at low frequencies.

In the search for the determination of dielectric responses, two comparative and complementary measurement methods are often preferred. Here, dielectric spectroscopy in frequency and time domains were used. Although the spectroscopy in the time domain implies a DC voltage difference applied to a dielectric, it is possible to transpose the signal data from the time domain to the frequency domain and vice versa. Furthermore, the temporal method allows the conduction contribution to be unravelled from the data.

The two methods used here performed well. All the results are consistent and the complementarity was a success. The case we used is especially illustrative for nanodielectrics. The nanocomposite is made of polyethylene (PE), with nanoclay as an additive.

Theoretical Background

To palliate the shortcomings of measurements related to the "memory effect" of dielectrics, measurements of the dielectric responses in the time domain were carried out using a cycle composed of a succession of polarization and depolarization steps, so that the polarized current I_{pol} resulting from the application of a voltage step is followed by a depolarization current I_{depol} resulting from short-circuiting of the dielectric. A schematic view of the complete sequence is depicted in Figure 1 [2].
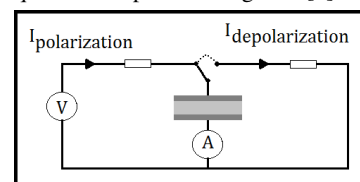

Fig. 1: Schematic view of the circuit to perform dielectric spectroscopy in the time domain.

For a plane-plane configuration as illustrated in Figure 1, the current resulting from the application of a voltage can be expressed as

$$I(t) = C_0 \left[\frac{\sigma_{dc}}{\varepsilon_0} U(t) + \frac{dU(t)}{dt} \right.$$
$$\left. + \int_0^\infty f(\tau) U(t-\tau) d\tau \right] \quad (1)$$
$$= I_{dc} + I_C + I_P.$$

with the first term being the direct conduction I_{dc}, the second term corresponding to the free charges and called the capacitive current I_C (with the assumption that the time constant associated with the resistance of the measuring circuit, cables, electrodes and voltage source is negligible), and the third term corresponding to the current I_p stemming from the polarization mechanisms.

Considering the application of a voltage step U_0 during a polarization time t_{pol} followed by a short-circuit, let us define $U(t)$ so that [3]

$$U(t) = \begin{cases} 0 & t < 0 \\ U_0 & 0 \le t < t_{pol} \\ 0 & t \ge t_{pol} \end{cases} \quad (2)$$

Then, the polarization and depolarization currents can be expressed as

$$I(t) = \begin{cases} 0 & t < 0 \\ I_{pol}(t) & 0 \le t < t_{pol} \\ I_{depol}(t) & t \ge t_{pol} \end{cases} \quad (3)$$

with

$$\frac{I_{pol}(t)}{C_0 U_0} = \frac{\sigma_{dc}}{\varepsilon_0} + \delta(t) + f(t)$$
$$\frac{I_{depol}(t)}{C_0 U_0} = -[\delta(t - t_{pol}) \qquad (4)$$
$$+ f(t - t_{pol}) - f(t)]$$

It is worth noting that $f(t)$, which represents the memory effect, tends to a negligible value for sufficiently long polarization times. Formulating equation Eq. (3), neglecting the memory effect and identifying various current denominations, we have

$$I_{pol}(t) = I_{dc} + I_c(t) + I_p(t)$$
$$I_{depol}(t) = -I_c(t) - I_p(t) \qquad (5)$$

We can extract the conduction current I_{dc} and then obtain the conductivity σ_{dc} of the sample by adding the polarization current I_{pol} to the depolarization current I_{depol} for any given time.

This gives

$$\sigma_{dc} = \frac{\varepsilon_0}{U_0 C_0} \cdot I_{dc}$$
$$= \frac{\varepsilon_0}{U_0 C_0} \cdot (I_{pol}(t) + I_{depol}(t))$$
$$\forall t \in [0, t_{pol}] \qquad (6)$$

The American Society for Testing and Materials has proposed a standard, known as D257 [4], which proposes a simplified protocol to measure the resistivity of insulating materials. That protocol is used to calculate the conductivity, by monitoring the current after a fixed polarization time (about 5 minutes). However, the ASTM protocol does not take into account the current bound to the mechanisms of residual polarization, and this can seriously compromise the quality of the measurement. Measuring the conductivity by means of Eq. (6) largely alleviates this drawback.

For linear dielectrics, it is possible to transpose the measurements taken in the time domain towards the frequency domain and vice versa, because the temporal response is connected to the complex susceptibility by a Fourier transform. The combination of the temporal and frequential spectroscopies allows the constraints of each of the measurement techniques to be somewhat overcome and to obtain supplementary information on the dielectric material under investigation [5].

Among the additional achievements possible with our proposed method are the verification of the linearity of the dielectric properties versus the electric field, the extension of the frequential domain toward the low frequencies for short acquisition times and the differentiation of the imaginary permittivity from the conductivity of the dielectric. It is worth mentioning that the mechanisms of charge injection and dispersion at low frequencies (charge transport) are non-linear phenomena and therefore cannot be transposed from one domain to another without altering their nature.

Three approaches can be used to transpose the data obtained in the time domain: the numerical Fourier transform, numerical curve fitting using a function with an analytical Fourier transform, and the Hamon approximation. However, since the po-

larization and depolarization currents are strongly non-periodic and measured over a large time period, the numerical Fourier transform does not allow (in general) the perfect transformation of the data into the frequency domain.

The analytical Fourier method is based on fitting the data with a curve so that the data can be transposed from the time domain to the frequency domain [6]. The transform allows the real and imaginary permittivity of the dielectric to be obtained via the Kramers-Kronig relations. However, its use presumes that the mechanisms of polarization and conduction can be identified *a priori*. For the slower polarization processes, Jonscher [7, 8] proposed that the response function $f(t)$ corresponding to the transition at a time between two different polarization mechanisms expresses itself under the shape of the "universal answer" as

$$f(t) = \frac{A}{\left(\frac{t}{\tau}\right)^m + \left(\frac{t}{\tau}\right)^n} \qquad (7)$$

where A, m and n are constants, and $0 < m < 1$ and $0 < n < 2$. Since this function does not have an analytical Fourier transform, Helgeson [6] proposes a modification of equation (7) so that the response function $f(t)$ contains one, while remaining asymptotically equal to the universal response as

$$f(t)/A = \exp\left(-\frac{t}{\tau}\right) \times \left(\frac{t}{\tau}\right)^{-m}$$
$$+ \left(1 - \exp\left(-\frac{t}{\tau}\right)\right) \times \left(\frac{t}{\tau}\right)^{-n} \qquad (8)$$

where A, m and n are constants, and $0 < m < 1$ and $0 < n < 2$. The analytical Fourier transform in question can then be expressed as

$$\frac{\chi^* - \chi_\infty}{A} = \frac{\tau^m \cdot \Gamma(1-m)}{\left(\frac{1}{\tau} + j\omega\right)^{1-m}}$$
$$- \frac{\tau^n \cdot \Gamma(1-n)}{\left(\frac{1}{\tau} + j\omega\right)^{1-n}} \qquad (9)$$
$$+ \frac{\tau^n \cdot \Gamma(1-n)}{(j\omega)^{1-n}}$$

with $\Gamma(x)$ representing the Gamma function and j the imaginary number. Thus, by separating the complex susceptibility $\chi^*(\omega)$ into real and imaginary parts, it is possible to transpose the response function $f(t)$

of the dielectric towards the dielectric frequency response. If many mechanisms interact in the dielectric response (polarization, dispersion at low frequency, etc.), it is necessary to identify each one, since the general response function is a sum of the individual mechanism response functions. This is also the case for complex susceptibility that is the result of the summation of several contributions. The term χ_∞ was added to equation (9) in order to take into account the contribution of polarization at high frequencies. Therefore, it is necessary to evaluate this factor at a common frequency-value for the measuring techniques in both the frequency and the time domains.

The Hamon approximation allows the measured value of the imaginary permittivity ε''_{mes} to be approximated from the measurement of polarization and depolarization currents with the time domain spectroscopy technique. The approximation is based on the hypothesis that the response function can be modelled as a series of power functions, $f(t) = A \cdot t^{-n}$, n being constant for a certain time range [9]. For $0.3 < n < 1.2$, this brings about on the approximation of ε''_{mes}, with an error of less than 3 %. The maximal error at the junction of two parts is less than 15 % for the worst case, and is usually less than 5 %. Setting $\omega\tau = 0.63$, the Hamon approximation takes the form

$$\varepsilon''_{mes} = \frac{i(t)}{\omega C_0 U_0} \qquad (10)$$

with $i(t)$ representing, according to an operator's choice, the polarization I_{pol} or depolarization I_{depol} current. This flexibility allows the contribution from the conductivity σ_{dc} in the

unravelling of the imaginary permittivity ε''_{mes} to be considered (or not). Furthermore, this approximation is very simple to implement and makes it possible to gain one decade in frequency with respect to that obtained using an analytical Fourier transform, since the factor $\omega\tau = 0.63$ (equivalent to $f \approx 0.1/\tau$) essentially gives access to results pertaining to the imaginary permittivity for frequencies at (or reaching) a decade lower.

Measurements: Techniques, Results and Discussion

Time domain spectroscopy and conductivity measurements were conducted using a two-active electrode setup and an electrometer (Keithley, model 6517B [10]). The sample holder consisted of two conductive rubber electrodes, with the measuring electrode guarded by a ring electrode. A step voltage of a maximum of 1000 V was applied across the sample and the polarization currents and depolarization current were monitored at the rate of 1 datum/s. Figure 2 shows the charge and the discharge currents in a log-log plot for a 5 wt% LLDPE/nanoclay sample with a diameter of 63.5 mm and a thickness of 560 μm. The applied voltage was 800 V, yielding a geometrical field of 1.4 kV/mm. The time is reset to zero when the electrodes are short-circuited and the discharge current is monitored. The acquisition time for each single measurement was defined by commercial software at (1 ± 0.05) s. This incertitude on the exact acquisition time has a direct impact on the calculation of the direct current conductivity as de-

fined by Eq. (6).

Figure 3 shows the direct conduction current calculated for each acquisition time. Since the polarization and depolarization currents are very close for times shorter than 100 s, there is a large variation in the magnitude of the conduction current. For longer times, the calculated value stabilizes to an almost steady state value of 5 pA. The inset of Figure 3 is an enlargement of the conduction current for the time window from 100 s to 10000 s. The apparent increase of the conductivity for times longer than 1600 s is due to the memory effect (the last term in the third equation of Eq. (3)). To minimize the influence of the memory effect, the conductivity should be calculated using the average value for times between 100 s and 1000 s.

Figure 4 shows the experimental material dielectric response function, $f(t)$, and the least square fitting of Eq. (8). It is clear that this equation is in good agreement with the experimental data. This is a required condition in order to ensure that the analytical Fourier transform can accurately describe the material frequency domain response. The frequency-domain measurements were conducted in a frequency range from 100 μHz to 3 MHz with a 3 V sinusoidal voltage applied across the sample.

Figure 5 shows the real and the imaginary parts of the complex permittivity as a function of frequency for the frequency-domain measurements and for the time-domain measurements converted into the frequency domain with both the Hamon approximation and the analytical Fourier Transform.
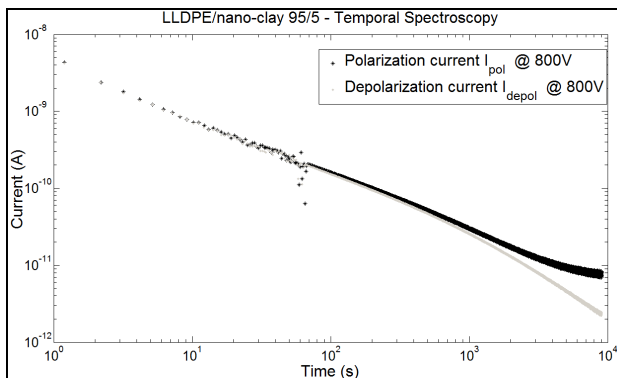

Fig. 2: Polarization and depolarization currents as a function of time for a 5 wt% LLDPE/clay nanocomposite at 1.4 kV/mm.
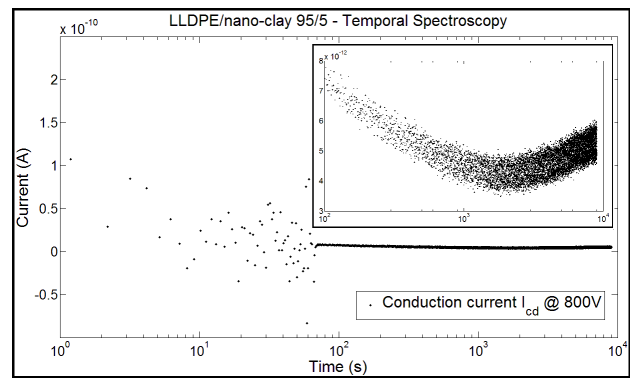

Fig. 3: Direct conduction current at 1.4 kV/mm as defined by Eq. (6) for a 5 wt% LLDPE/clay nanocomposite.
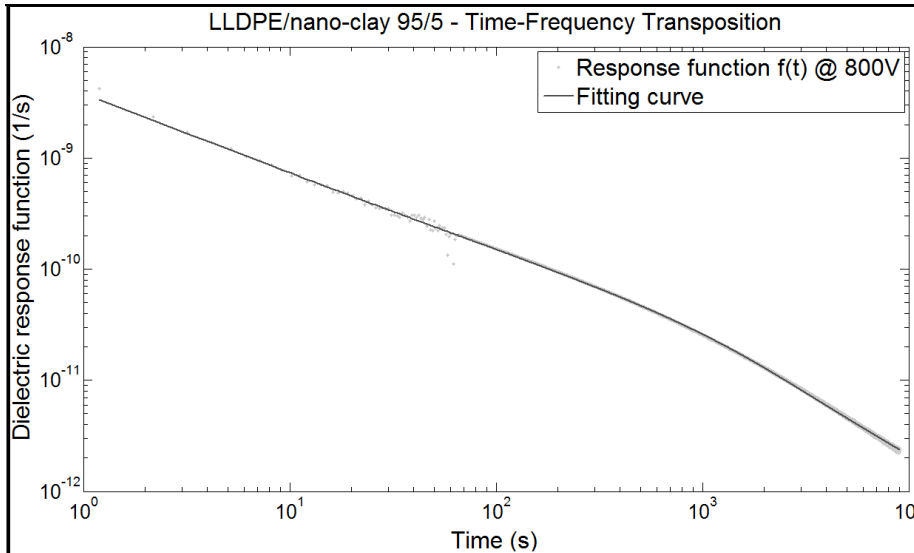
Fig. 4: Experimental dielectric response function (diamonds) and the least square fitting of Eq. (8) for a 5 wt% LLDPE/clay nanocomposite under a 1.4 kV/mm DC electrical field.
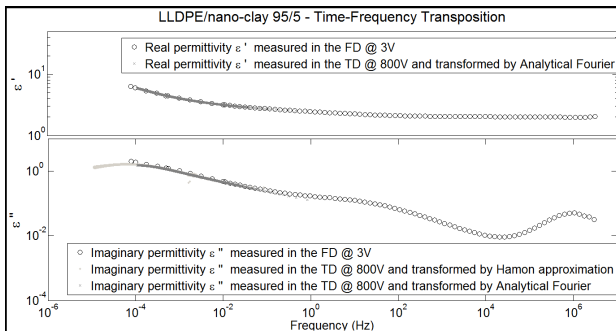

Fig. 5: Real and imaginary parts of the complex permittivity for a 5 wt% LLDPE/clay nanocomposite.
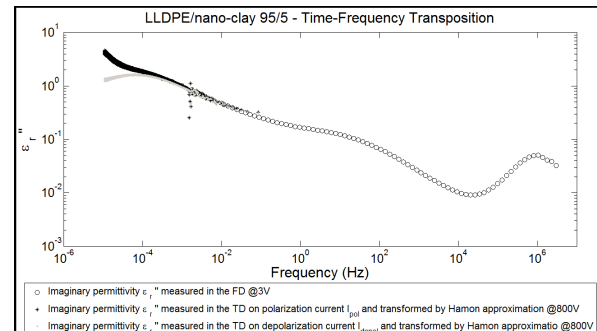

Fig. 6: Imaginary permittivity as a function of frequency for frequency domain measurements and for the charge and discharge currents converted using the Hamon approximation.

It can be seen that both time-domain and frequency-domain measurements are in very good agreement despite the fact that these measurements were conducted at a very different electrical field (the field was 250 times higher for the measurements in the time-domain) which indicates that the material is a linear dielectric up to 1.4 kV/mm. Furthermore, the analytical Fourier transform from the time domain data was found appropriate to obtain the real as well as the imaginary part of the permittivity. However, for frequency below 150 µHz, both transformation techniques underestimate the value of the imaginary part of the permittivity since the discharge current was used, and so the contribution of the direct conductivity was not taken into consideration. In addition, the memory term in Eq. (3) leads to a downward curvature of the discharge current at the end of the curve which leads to a decrease of the resulting imaginary permittivity. The memory effect

in the time domain can be compensated for by various numerical techniques [3]. Figure 6 shows the variation of the imaginary part of the permittivity as a function of frequency for the 5 wt% LLDPE/nanoclay sample, where the time-domain data is converted into the frequency domain with the Hamon approximation for both the charge and the discharge currents. By comparing the Hamon approximation for the charge and discharge currents, one can estimate the contribution of the direct conductivity. It can also be observed that there is a very good agreement between the transformation of the charge current and the frequency-domain data.

Finally, a high frequency relaxation peak appears in the vicinity of 1 MHz. This peak is not related to the material's dielectric response; rather, it is related to a contribution from the rubber electrodes [11–13]. The other relaxation peaks at lower frequencies are interfacial polarization peaks that are closely related to the material microstructure. A more detailed discussion on this subject can be found elsewhere [14].

Closing Remarks

This paper offers a detailed and comprehensive review of a formulation for transposing polarization data from time to frequency domains. Knowledge of the dielectric response of polarizable solid materials is an essential foundation to support the development of high-performance HV insulation systems and sustain the development of advanced dielectrics, such as nanodielectrics, which explains the necessity to master the accessibility, accuracy and reproducibility of its measurement. The main contribution of this paper is to demonstrate the successful use of the two techniques, namely dielectric spectroscopy in time and frequency domains, to produce excellent data combined with exemplary complementarity. Finally, this demonstration

was achieved with a nanodielectric, an emerging class of dielectrics with a great potential for improving insulation systems.

Acknowledgment

References

[1] M.F. Fréchette, M. Trudeau, H.D. Alamdari and S. Boily, Proc. IEEE Conf. on Elect. Insul. and Dielec. Pheno., Kitchener, Ontario, Canada, Oct. 14-17 (2001). An extended version was subsequently archived in IEEE Trans. on Dielectr. and Electr. Insul., **11**, 808-818, 2004.

[2] A. Toureille, Techniques de l'ingénieur. Mesures et contrôle, no R1115v2, 1-18, 2009.

[3] É. David, R. Soltani and L. Lamarre, IEEE Trans. Dielectr. Electr. Ins., **17**, 1461-1469, 2010.

[4] American Society for Testing and Materials, *Standard Test Methods for DC Resistance or Conductance of Insulating Materials*. ASTM D257-07 Standard. West Conshohocken (PA) 2007, p. 18.

[5] Schaumburg, G. 1997. Novocontrol, Dielectrics Newsletter. no 8, p. 5-10. http://www.novocontrol.de/newsletter/DNL08.PDF.

[6] A. Helgeson. 2000. "Analysis of dielectric response measurement methods and dielectric properties of resin-rich insulation during processing". Stockholm, Kungl Tekniska Högskolan, 221 p.

[7] A.K. Jonscher, *Dielectric relaxation in solids*, London (UK): Chelsea Dielectric Press 1983, 380 p.

[8] A.K. Jonscher, *Universal relaxation law*. London: Chelsea Dielectrics Press 1996, 415 p.

[9] Hamon, B.V, Proc. IEE. **99**, 151-155, 1952.

[10] Keithley Instruments Inc. 2010. "6517B: "Electrometer/High Resistance Meter". 4 p. http://www.keithley.com/data?asset=51992.

[11] Meier, J G., J W. Mani and M. Klüppel, Phys. Rev. B, **75**, 054202, 2007.

[12] J.G. Meier, M. Klüppel, Macromol. Mater. Eng. **293**, 12-38, 2008.

[13] R.N. Capps, J. Burns, J. Non-Cryst. Solids, **131-133**, 877-882, 1991.

[14] É. David, C. Daran-Daneau, M.F. Fréchette, B. Zazoum, A.D. Ngô, S. Savoie, International Symposium on Electric Insulation, San Juan, 2012.

C. Daran-Daneau[1], E. David[1], M. Fréchette[2], and S. Savoie[2]
[1]École de technologie supérieure (ETS), Québec, Canada
[2]Institut de recherche d'Hydro-Québec (IREQ), Varennes, Québec, Canada

Conference Announcement BDS 2012: "Broadband Dielectric Spectroscopy and its Applications"

During the past two decades, Broadband Dielectric Spectroscopy (BDS) has become a major spectroscopic tool alongside Nuclear Magnetic Resonance (NMR) and Fourier Transform Infra-Red (FTIR) spectroscopy. The entire spectral range from ultraslow (<1 mHz) to Terahertz frequencies can be covered without any gap using modern equipment. This grants unique access to a wealth of information about molecular and collective dipolar fluctuations, charge transport as well as interfacial polarization in diverse categories of materials spanning the scale from electrically conducting to entirely insulating systems. Consequently, numerous basic and applied topics are studied by dielectric techniques. The conference provides a platform to discuss these exciting developments. In detail, the following topics will be addressed:

1.) BDS in relation to other spectroscopic or scattering techniques (Neutron, X-ray, and Light scattering, NMR, IR-spectroscopy, DSC and AC-calorimetry, mechanical and ultrasound spectroscopy), 2.) Terahertz spectroscopy, 3.) Theory of dielectrics, 4.) BDS in relation to Electrochemistry, 5.) Glassy dynamics and its scaling, 6.) Rotational and translational diffusion in conducting glasses and Ionic Liquids, 7.) Electrode and Maxwell-Wagner polarization, 8.) Charge transport and glassy dynamics in confining geometries of different dimensionality, 9.) Dielectric properties of biological systems, 10.) Industrial applications of BDS
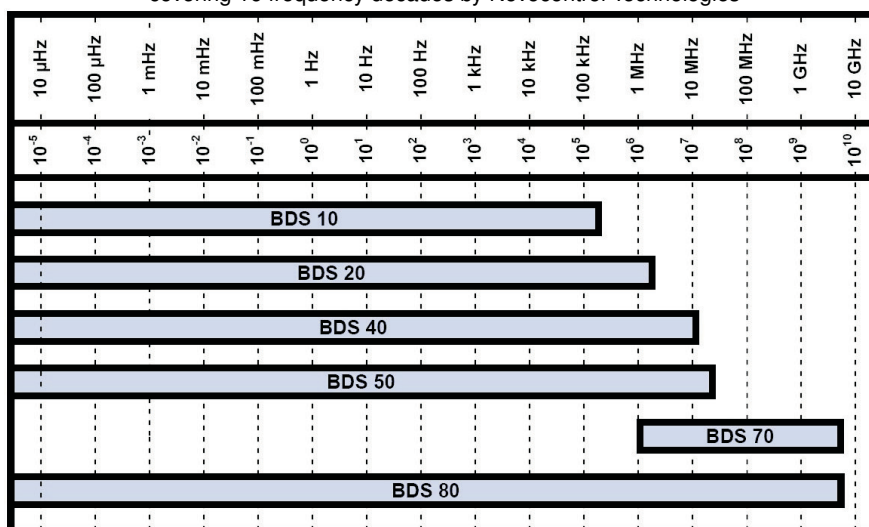
The List of confirmed invited speakers includes:

S. Abd-El-Messieh (Egypt), A. Alegria (Spain), T. Andachi (Japan), J. Bartos (Slovakia), P. Ben Ishai (Japan), R. Böhmer (Germany), G. Boiteux (France), V. Boucher (Spain), D. Cangialosi (Spain), S. Capaccioli (Italy), S. Cerveney (Spain), W. Coffey (Ireland), R. Colby (USA), J. Colmenero (Spain), T. Ezquerra (Spain), Y. Feldman (Israel), G. Floudas (Greece), D. Fragiadakis (USA), K. Fukao (Japan), K. Gainaru (Germany), R. Gerhard (Germany), M. Havenith-Newen (Germany), I. Hayut (Israel), R. Hilfer (Germany), H. Huth (Germany), G. Johari (Canada), K. Kawase (Japan), R. Kisiel (Poland), F. Kremer (Germany), A. Kumbharkhane (Inia), A. Kyritsis (Greece), A. Loidl (Germany), P. Lunkenheimer (Germany), A. Lyashchenko (Russia), K. Ngai (Italy), M. Massalska-Arodz (Poland), B. Mazzero (USA), M. Nakanishi (USA), S. Napolitano (Belgium), R. Nigmatullin (Kazan), G. Niklasson (Sweden), A. Nogales (Spain), R. Nozaki (Japan), M. Paluch (Poland), D. Prevosto (Italy), R. Richert (USA), A. Robitzki (Germany), B. Roling (Germany), J. Runt (USA), A. Saad (Egypt), J. Sangoro (Germany), A. Schönhals (Germany), Chr. Schröder (Austria), A. Serghei (France), L. Singh (USA), A. Sokolov (USA), H. Svajdlenkova (Slovakia), J. Ulanski (Poland), M. Wübbenhorst (Belgium), N. Yamamoto (Japan)

Conference chairman:
Friedrich Kremer
Universität Leipzig
Institut für Experimentelle Physik I
Linnéstraße 5
04103 Leipzig, Germany
For further information:
BDS2012.uni-leipzig.de

OVERVIEW

BROADBAND DIELECTRIC AND IMPEDANCE SPECTROSCOPY
covering 16 frequency decades by Novocontrol Technologies

Factory and Head Office

Germany
Novocontrol Technologies GmbH & Co. KG
Obererbacher Straße 9
56414 Hundsangen/GERMANY
Contact: Dr. Dirk Wilmer

Phone: +49 6435 9623-0
Fax: +49 6435 9623-33
Mail: novo@novocontrol.de
Web: www.novocontrol.de

Agents

USA/Canada
Novocontrol America Inc.
Wake Forest, NC 27587 / USA
Toll free: +1 866 554 9904
Phone: +1 919 554 9904
Fax: +1 919 573 0373
Mail: novocontrolusa@earthlink.net
Contact: Mr. Joachim Vinson, PhD

Japan
Morimura Bros. Inc.
Minato-Ku, Tokyo 105
Phone: +81 3-3502-6440
Fax: +81 3-3502-6437
Mail: m-amano@morimura.co.jp
Contact: Mr. Mizuki Amano

People's Republic of China
GermanTech Co. Ltd
Beijing, 100083
Phone: +86 10 82867920/21/22
Fax: +86 10 82867919
Mail: contact@germantech.com.cn
Contact: Mrs.Yue Tian

South Korea
HI Corporation
Anyang-shi, Kyungki-Do, Korea
Phone: +82 31 479 6250
Fax: +82 31 479 6255
Mail: hicorpkim@chol.com
Contact: Mr. Jason Kim

India
A-Tech Systems
Mumbai 400 080
Phone: +91 22 2294 3222 and 2164 0515
Fax: +91 22 2164 0525
Mobile: +91 22 9322 255 717
Email: arvind.atech@gmail.com
contact: Mr. Arvind Panchal

India
Sinsil International HO
Mumbai 400 607
Mobile: +91 9833011933
Mobile: +91 9870225777
Mail: sinsilmumbai@gmail.com
Contact: Dr. K. Ramesh

Brasil
Instrutécnica Comércio Representações e Serviços Ltda
13084-643 Campinas SP
Phone: +55 19 3289 9649
Fax: +55 19 3343 7770
Email: vendas@instrutecnica.com.br
contact: Dr. Ricardo Mendes

Greece
Vector Technologies Ltd.
15234 Halandri, Athens
Phone: +30 210 685 8008
Fax: +30 210 685 8118
Mail: info@vectortechnologies.gr
Contact: Mr. Vouvounas

Editor: Dirk Wilmer. Abstracts and papers are always welcome. Please send your manuscript to the editor.